Mathematical Biosciences and Engineering

http://www.aimspress.com/journal/mbe

MBE, 20(1): 1519–1537.
DOI: 10.3934/mbe.2023069
Received: 30 July 2022
Revised: 14 October 2022
Accepted: 16 October 2022
Published: 03 November 2022

Research article

Bifurcation analysis of a sheep brucellosis model with testing and saturated culling rate

Yongbing Nie[1], Xiangdong Sun[2], Hongping Hu[1] and Qiang Hou[1,*]

[1] School of Mathematics, North University of China, Taiyuan, Shanxi 030051, China
[2] China Animal Health and Epidemiology Center, Qingdao, Shandong 266032, China

* **Correspondence:** Email: houqiang200207@163.com.

Abstract: Testing-culling is a very effective measure for the prevention and control of animal diseases. In this paper, based on sheep brucellosis control policies and animal testing characteristics and considering the limitation of culling resources, a dynamic model is established to study the impact of testing-culling measure. Theoretical analysis reveals that the model may have one or three positive equilibria. The equilibrium in the middle is always unstable, and the model shows saddle-node bifurcation, generalized Hopf bifurcation and Bogdanov-Takens bifurcation. Moreover, the theoretical results are verified via numerical analysis. These results reveal that testing and culling strategies can induce complex transmission dynamics that can help us develop appropriate prevention and control measures for animal brucellosis.

Keywords: brucellosis; animal testing; saturated culling rate; stability; bifurcation

1. Introduction

Brucella is a gram-negative, non-motile coccobacillus that can parasitize various types of livestock and cause brucellosis [1]. Brucellosis can be transmitted to susceptible humans and animals mainly through contact with infected animals or ingestion of pathogens from the environment. Brucellosis can cause miscarriage and orchitis in animals and fever, fatigue, joint pain and other symptoms in humans [2]. Brucellosis is found all over the world, and nearly 500,000 new cases are recorded every year [3]. The brucellosis epidemic not only endangers human health but also affects animal husbandry, which has a large adverse effect on economic development and public health [4].

For the prevention and control of animal brucellosis, vaccination, disinfection and testing-culling are the main measures. Many authors have studied the impact of vaccination on the spread of animal brucellosis, and quantitative results have been obtained [5, 6]. However, a 100% vaccination rate of animals is difficult to achieve, and some vaccines have negative effects. For example, in Korea,

vaccination of cattle with RB51 caused side-effects, including abortion, premature birth and a reduced milk yield [7]. In other words, brucellosis cannot be eradicated only by vaccination, and other measures should be taken to control animal brucellosis. Although testing and culling measures are difficult to implement in some developing countries because of the high economic cost, they can eliminate animal diseases. For example, bovine brucellosis in New Zealand caused heavy losses to the livestock industry and was eventually eliminated through testing and culling measures [8]. Testing and culling measures have been used to prevent and control brucellosis and have significantly reduced the spread of this disease in most Southeast Asian countries [9]. Therefore, testing and culling measures are necessary for brucellosis eradication.

Recent studies on the impact of testing and culling measures have contributed to the understanding of the effectiveness of brucellosis control measures [10–14]. However, these studies mainly focus on the impact of culling measures, and the impact of testing principles and processes on animal brucellosis is still not well researched, which is not conducive to the understanding of the impact of testing behavior and leads to neglect of this risk factor in mathematical modelling. In practice, if an infected animal is found in one place, then all animals in that place will be tested. For example, in Inner Mongolia, China, sheep are numerous, and if an infected sheep is found in one place (a township is treated as a unit), all sheep are tested. Importantly, because of the larger number of sheep, in general, a certain proportion of animals are tested per unit time. In addition, culling resources derived from government supplies may be limited because of the many positive animals. On the basis of these two risk factors and ignoring the contagion of environmental pathogens, a sheep brucellosis model is established:

$$\begin{cases} \frac{dS}{dt} = A - \beta S I - \mu S, \\ \frac{dI}{dt} = \beta S I - (\sigma + \mu) I - m\phi I I_d, \\ \frac{dI_d}{dt} = m\phi I I_d + \sigma I - \mu I_d - \frac{c I_d}{\alpha + I_d}, \end{cases} \tag{1.1}$$

where $S(t)$ represents the susceptible population, $I(t)$ is the infectious population and $I_d(t)$ is the infectious population with clinical features or found by serological testing. Let A be the constant recruitment rate. β and μ are the infection rate and the natural death rate, respectively. σ is the rate of infected animals with clinical features. m is the fraction of positive animals found by testing. ϕ is defined as the testing rate, the number of animals tested is ϕN per unit of infectious animals $I_d(t)$, thus the number of infected animals that have been found through testing is $m\phi N \frac{I}{N} I_d = m\phi I I_d$. c represents the maximal supply of culling resources and α is half-saturation constant, measuring the efficiency of the supply of culling resources. The parameters of the model are positive constants.

The motivation for this article is to investigate the impact of restricted culling resources on the dynamics of brucellosis transmission. The rest of this paper is arranged as follows. The basic properties of the model are given in Section 2. In Section 3, the stability of equilibria, saddle-node bifurcation, Hopf bifurcation and Bogdanov-Takens bifurcation of codimension 2 are analyzed. In Section 4, the theoretical results are verified by numerical simulation. Finally, conclusions and discussions are given in Section 5.

2. Basic properties of model

For model (1.1), one can find that

$$\begin{aligned}\frac{d(S+I+I_d)}{dt} =& A-\mu S-\mu I-\mu I_d-\frac{cI_d}{\alpha+I_d}\\ \leq& A-\mu(S+I+I_d),\end{aligned}$$

it follows that

$$\lim_{t\to\infty}\sup(S+I+I_d)\leq\frac{A}{\mu}.$$

So the set

$$\Omega=\{(S,I,I_d)\in R^3: S,I,I_d\geq 0, S+I+I_d\leq\frac{A}{\mu}\}$$

is the positively invariant set of model (1.1).

It is easy to verify that model (1.1) has a disease-free equilibrium $E_0=(\frac{A}{\mu},0,0)$. According to the next generation matrix method [15], the basic reproduction number is given by

$$R_0=\frac{\beta A}{\mu(\sigma+\mu)}.$$

For the existence of the endemic equilibrium $E(S^*,I^*,I_d^*)$ of model (1.1), the following equations are given:

$$\begin{cases}A=\beta SI+\mu S,\\ \beta SI=(\mu+\sigma)I+m\phi I_dI,\\ m\phi I_dI+\sigma I=(\mu+\frac{c}{\alpha+I_d})I_d.\end{cases}\tag{2.1}$$

According to the above equations, S^* and I^* can be expressed as functions of I_d^*. That is,

$$S^*=\frac{\mu+\sigma+m\phi I_d^*}{\beta},\ \ I^*=\frac{-m\phi\mu I_d^*+\mu(\mu+\sigma)(R_0-1)}{\beta(m\phi I_d^*+\mu+\sigma)},$$

where I_d^* is given by the equation

$$f(I_d^*)=B_0{I_d^*}^3+B_1{I_d^*}^2+B_2I_d^*+B_3=0,\tag{2.2}$$

where

$$\begin{aligned}B_0=&-m\mu\phi(m\phi+\beta)<0,\\ B_1=&\mu m\phi(\mu+\sigma)(R_0-1)-\mu(\alpha m\phi+\sigma)(m\phi+\beta)-\beta\mu^2-\beta cm\phi,\\ B_2=&\mu(\mu+\sigma)(\alpha m\phi+\sigma)(R_0-1)-\beta(\mu+\sigma)(\alpha\mu+c)-\alpha m\mu\phi\sigma,\\ B_3=&\alpha\sigma\mu(\mu+\sigma)(R_0-1).\end{aligned}$$

Note that $I^*>0$ and $R_0>1$, then $I_d^*<I_c^*=\frac{(\mu+\sigma)(R_0-1)}{m\phi}$.

Let

$$B=B_1^2-3B_0B_2,\ \ C=B_1B_2-9B_0B_3,\ \ D=B_2^2-3B_1B_3,\ \ \Delta=C^2-4BD.$$

Based on the Descarte's rule of signs, the following cases can be obtained:
Case 1: $B_2 > 0$ or $B_1 < 0, B_2 < 0$. There is a unique positive root of $f(I_d^*) = 0$.
Case 2: $B_1 > 0, B_2 < 0$. Similar to the method in [16], the following results can be obtained:
(a) $\Delta > 0$, there is a unique positive root of $f(I_d^*) = 0$;
(b) $\Delta = 0$, there are two positive roots of $f(I_d^*) = 0$;
(c) $\Delta < 0$, there are three positive roots of $f(I_d^*) = 0$.
To sum up the above results, the following conclusions are derived.

Theorem 1. Assumed that $R_0 > 1$. If $B_2 > 0$ or $B_1 < 0, B_2 < 0$ or $B_1 > 0, B_2 < 0, \Delta > 0$, model (1.1) has a unique endemic equilibrium E_1; if $B_1 > 0, B_2 < 0, \Delta = 0$, model (1.1) has two endemic equilibria E_1 and E_*, E_* is an endemic equilibrium of multiplicity 2; if $B_1 > 0, B_2 < 0, \Delta < 0$, model (1.1) has three endemic equilibria E_1, E_2 and E_3.

3. Dynamic properties of model

In this section, the stability of equilibria and the local bifurcation of model (1.1) are analyzed, it is of great significance for the prevention and control of brucellosis.

3.1. Stability of equilibria

In this subsection, the global stability of disease-free equilibrium and the local stability of endemic equilibria are analyzed. The following results are first given:

Theorem 2. For model (1.1), if $R_0 \leq 1$, then E_0 is globally asymptotically stable.

Proof. The Jacobian matrix of model (1.1) at E_0 takes the form

$$J_{E_0} = \begin{pmatrix} -\mu & -\frac{\beta A}{\mu} & 0 \\ 0 & \frac{\beta A}{\mu} - \mu - \sigma & 0 \\ 0 & \sigma & -\mu - \frac{c}{\alpha} \end{pmatrix},$$

then J_{E_0} has eigenvalues $\lambda_1 = -\mu, \lambda_2 = -(\mu + \frac{c}{\alpha})$ and $\lambda_3 = (R_0 - 1)(\sigma + \mu)$. Therefore, E_0 is locally asymptotically stable if $R_0 < 1$ and E_0 is unstable if $R_0 > 1$.

Next, when $R_0 \leq 1$, define the Lyapunov function L as follows:

$$L = S - S_0 - S_0 \ln \frac{S}{S_0} + I.$$

It can be concluded that

$$\begin{aligned} \dot{L} &= (1 - \frac{S_0}{S})\frac{dS}{dt} + \frac{dI}{dt} \\ &= (1 - \frac{S_0}{S})(A - \beta S I - \mu S) + \beta S I - (\mu + \sigma)I - m\phi I I_d \\ &\leq \mu S_0(2 - \frac{S_0}{S} - \frac{S}{S_0}) + (R_0 - 1)(\mu + \sigma)I. \end{aligned}$$

Thus, $\dot{L} \leq 0$. Note that the equality $\dot{L} = 0$ means $S = S_0$ and $I = 0$, it implies that E_0 is the maximum invariant set of model (1.1) in the set $\{\dot{L} = 0\}$. Therefore, E_0 is globally asymptotically stable by LaSalle's invariance principle. □

The Jacobian matrix at any endemic equilibrium $E(S^*, I^*, I_d^*)$ is given by

$$J_E = \begin{pmatrix} a & b & 0 \\ d & 0 & f \\ 0 & h & l \end{pmatrix}, \tag{3.1}$$

where

$$a = -\frac{A}{S^*}, \ \ b = -\beta S^*, \ \ d = \beta I^*, \ \ f = -m\phi I^*,$$
$$h = \beta S^* - \mu, \ \ l = \frac{A - \mu S^* - \mu I^* - \mu I_d^*}{\alpha + I_d^*} - \frac{\sigma I^*}{I_d^*}.$$

The characteristic equation can be written as

$$\lambda^3 + \alpha_1 \lambda^2 + \alpha_2 \lambda + \alpha_3 = 0, \tag{3.2}$$

where

$$\alpha_1 = \frac{1}{(\alpha + I_d^*)S^* I_d^*}((A + \mu S^*){I_d^*}^2 + (\mu {S^*}^2 + (\mu I^* + \sigma I^* - A)S^* + \alpha A)I_d^* + \alpha\sigma S^* I^*),$$
$$\alpha_2 = \frac{1}{(\alpha + I_d^*)S^* I_d^*}((S^*(\beta(m\phi + \beta)S^* - m\mu\phi)I^* + \mu A){I_d^*}^2 + ((\beta\alpha(m\phi + \beta){S^*}^2 - m\mu\phi\alpha S^*$$
$$+ A(\sigma + \mu))I^* + \mu S^* A - A^2)I_d^* + \alpha\sigma A I^*),$$
$$\alpha_3 = \frac{1}{(\alpha + I_d^*)S^* I_d^*}((\beta m\phi A S^* + \beta^2 \mu {S^*}^2 - m\mu\phi A){I_d^*}^2 + (-{S^*}^2(-\mu I^* - \sigma I^* - \mu S^* + A)\beta^2$$
$$+ m\phi\alpha\beta A S^* - m\mu\phi\alpha A)I_d^* + \alpha\sigma\beta^2 I^* {S^*}^2)I^*.$$

From Eq (2.2), we can represent the coefficient α_3 as a function on I_d^* as follows:

$$\alpha_3(I_d^*) = -\beta(m\phi I_d^* + \mu + \sigma)I^* f'(I_d^*). \tag{3.3}$$

It follows from Eq (2.2) that $f'(I_{d1}^*) < 0$, $f'(I_{d3}^*) < 0$ and $f'(I_{d2}^*) > 0$ when E_1, E_2 and E_3 exist. That is, $\alpha_3(I_{d1}^*) > 0, \alpha_3(I_{d3}^*) > 0$ and $\alpha_3(I_{d2}^*) < 0$. Thus E_2 is unstable.

Let $\Delta(I_d^*) = \alpha_1(I_d^*)\alpha_2(I_d^*) - \alpha_3(I_d^*)$, the following results are derived.

Theorem 3. For model (1.1), the equilibrium E_2 is unstable when it exists. If $\alpha_1 > 0, \Delta(I_d^*) > 0$, the equilibria E_1 and E_3 is locally asymptotically stable when they exist.

Remark. If there is no serological test, the third equation of model (1.1) is independent of the other equations, and a general SI model can be obtained that has a disease-free equilibrium and an endemic equilibrium, both of which are globally asymptotically stable.

3.2. Bifurcation analysis

In this subsection, the conditions for the occurrence of saddle-node, Hopf and Bogdanov-Takens bifurcations are given, which are necessary to understand the impact of testing-culling.

3.2.1. Saddle node bifurcation

Based on the Theorem 1, it is easy to verify that there are two endemic equilibria when $\Delta = 0$, which implies that the characteristic Eq (3.2) has a simple zero eigenvalue at E_*. That is, model (1.1) may undergo a saddle-node bifurcation. In the following pages, a detailed analysis is given by choosing σ as the bifurcation parameter.

Let F_σ be the derivative of F with respect to σ, where $F = (F_1, F_2, F_3)^{\mathrm{T}}$ is shown as follows:

$$\begin{cases} F_1 \triangleq A - \beta S I - \mu S, \\ F_2 \triangleq \beta S I - (\sigma + \mu) I - m\phi I I_d, \\ F_3 \triangleq m\phi I I_d + \sigma I - \mu I_d - \frac{cI_d}{\alpha + I_d}. \end{cases}$$

Let V and W be the eigenvectors corresponding to the eigenvalue $\lambda = 0$ for J_{E_*} and $J_{E_*}^T$. Then they can be given by

$$V = \begin{pmatrix} V_1 \\ V_2 \\ V_3 \end{pmatrix} = \begin{pmatrix} \frac{-bl}{a} \\ l \\ -h \end{pmatrix}, W = \begin{pmatrix} W_1 \\ W_2 \\ W_3 \end{pmatrix} = \begin{pmatrix} \frac{-dl}{a} \\ l \\ -f \end{pmatrix},$$

where a, b, d, f, h, l are given in (3.1). Furthermore, one can get

$$F_\sigma(E_*; \sigma^*) = \begin{pmatrix} 0 \\ -I^* \\ I^* \end{pmatrix}$$

and

$$D^2 F(E_*; \sigma^*)(V, V) = \begin{pmatrix} -2\beta V_1 V_2 \\ 2\beta V_1 V_2 - 2m\phi V_2 V_3 \\ 2m\phi V_2 V_3 + \frac{2c\alpha}{(\alpha + I_d^*)^3} V_3^2 \end{pmatrix}.$$

It follows that

$$\begin{aligned} W^T F_\sigma(E_*; \sigma^*) &= (\mu + \frac{c\alpha}{(\alpha + I_d^*)^2}) I^* \neq 0, \\ W^T [D^2 F(E_*; \sigma^*)(V, V)] &= -\frac{2\beta^2 \mu S^*}{(\beta I^* + \mu)^2} (\frac{cI_d^*}{(\alpha + I_d^*)^2} - \frac{\sigma I^*}{I_d^*})^3 \\ &\quad + 2m\phi(m\phi I_d^* + \sigma)(\frac{cI_d^*}{(\alpha + I_d^*)^2} - \frac{\sigma I^*}{I_d^*})(\frac{cI_d^*}{(\alpha + I_d^*)^2} \\ &\quad - \mu - \frac{c}{\alpha + I_d^*}) + \frac{2cm\alpha\phi I^*(m\phi I_d^* + \sigma)^2}{(\alpha + I_d^*)^3}. \end{aligned}$$

Therefore, when $W^T [D^2 F(E_*; \sigma^*)(V, V)] \neq 0$, model (1.1) undergoes a saddle-node bifurcation at E_*.

3.2.2. Hopf bifurcation

In this subsection, Hopf and generalized Hopf bifurcations are considered. Let c as the bifurcation parameter, if there exists $c_1 > 0$ such that $\alpha_2(c_1) > 0$ and $\alpha_1(c_1)\alpha_2(c_1) = \alpha_3(c_1)$, the characteristic Eq (3.2) has a pair of pure imaginary eigenvalues $\pm i\sqrt{\alpha_2}$ and a real root $-\alpha_1$. For sufficiently small $\epsilon > 0$, when $c \in (c_1 - \epsilon, c_1 + \epsilon)$, the eigenvalues can be represented as

$$\lambda_1 = -\alpha_1(c),\ \lambda_2 = \omega(c) + iv(c),\ \lambda_3 = \omega(c) - iv(c).$$

Substituting λ_2 into Eq (3.2), the transversality condition of Hopf bifurcation can be obtained.

$$\operatorname{sign}\left\{\frac{\mathrm{d}\omega(c)}{\mathrm{d}c}\right\}_{c=c_1} = \operatorname{sign}\left\{\frac{\mathrm{d}(\alpha_1(c)\alpha_2(c) - \alpha_3(c))}{\mathrm{d}c}/(2\alpha_1^2(c) + \alpha_2(c))\right\}_{c=c_1} \neq 0.$$

Hence, model (1.1) shows a Hopf bifurcation when $c = c_1$.

Next, we calculate the first and second Lyapunov coefficients by using normal form theory in [17]. Let $x = S - S^*, y = I - I^*, z = I_d - I_d^*$, then the following system is obtained through the Taylor series about the origin.

$$\begin{cases} \frac{dx}{dt} = ax + by + a_{110}xy, \\ \frac{dy}{dt} = dx + fz + b_{110}xy + b_{011}yz, \\ \frac{dz}{dt} = hy + lz + c_{011}yz + c_{002}z^2 + c_{003}z^3 + c_{004}z^4 + c_{005}z^5 + O(|z|^6), \end{cases} \tag{3.4}$$

where a, b, d, f, h, l are given in (3.1), and

$$a_{110} = -\beta,\ b_{110} = \beta,\ b_{011} = -m\phi,\ c_{011} = m\phi,\ c_{002} = \frac{c\alpha}{(\alpha + I_d^*)^3},$$
$$c_{003} = -\frac{c\alpha}{(\alpha + I_d^*)^4},\ c_{004} = \frac{c\alpha}{(\alpha + I_d^*)^5},\ c_{005} = -\frac{c\alpha}{(\alpha + I_d^*)^6}.$$

Define $\omega = (x, y, z)^{\mathrm{T}}$, note that system (3.4) can be written as

$$\dot{\omega} = J\omega + F(\omega), \tag{3.5}$$

where

$$J = J_E,$$
$$F(\omega) = \frac{1}{2}B(\omega, \omega) + \frac{1}{3!}C(\omega, \omega, \omega) + \frac{1}{4!}D(\omega, \omega, \omega, \omega) + \frac{1}{5!}E(\omega, \omega, \omega, \omega, \omega) + O(|\omega|^6),$$

here

$$B(x, y) = \sum_{j,k=1}^{3} \frac{\partial^2 F(\omega)}{\partial\omega_j\partial\omega_k}\Big|_{\omega=0} x_j y_k = \begin{pmatrix} a_{110}(x_1y_2 + x_2y_1) \\ b_{110}(x_1y_2 + x_2y_1) + b_{011}(x_2y_3 + x_3y_2) \\ c_{011}(x_2y_3 + x_3y_2) + 2c_{002}x_3y_3 \end{pmatrix},$$

$$C(x, y, z) = \sum_{j,k,l=1}^{3} \frac{\partial^3 F(\omega)}{\partial\omega_j\partial\omega_k\partial\omega_l}\Big|_{\omega=0} x_j y_k z_l = \begin{pmatrix} 0 \\ 0 \\ -\frac{6c\alpha}{(\alpha+I_d^*)^4}x_3y_3z_3 \end{pmatrix},$$

$$D(x,y,z,v)=\sum_{j,k,l,r=1}^{3}\frac{\partial^4 F(\omega)}{\partial\omega_j\partial\omega_k\partial\omega_l\partial\omega_r}\Big|_{\omega=0}x_jy_kz_lv_r=\begin{pmatrix}0\\0\\\frac{24c\alpha}{(\alpha+I_d^*)^5}x_3y_3z_3v_3\end{pmatrix},$$

$$E(x,y,z,v,w)=\sum_{j,k,l,r,s=1}^{3}\frac{\partial^5 F(\omega)}{\partial\omega_j\partial\omega_k\partial\omega_l\partial\omega_r\partial\omega_s}\Big|_{\omega=0}x_jy_kz_lv_rw_s=\begin{pmatrix}0\\0\\-\frac{120c\alpha}{(\alpha+I_d^*)^6}x_3y_3z_3v_3w_3\end{pmatrix}.$$

It is easy to check that

$$Jq=\lambda q,\ J^{\mathrm{T}}p=\overline{\lambda}p,\ \langle p,q\rangle=1,$$

where

$$q=\begin{pmatrix}\frac{b}{i\sqrt{\alpha_2}-a}\\1\\\frac{h}{i\sqrt{\alpha_2}-l}\end{pmatrix},\ p=\frac{(a^2+\alpha_2)(l^2+\alpha_2)}{\alpha_2^2+(a^2+bd+fh+l^2)\alpha_2+(fh+l^2)a^2+bdl^2}\begin{pmatrix}\frac{d}{-i\sqrt{\alpha_2}-a}\\1\\\frac{f}{-i\sqrt{\alpha_2}-l}\end{pmatrix}.$$

By simple calculation

$$\begin{aligned}
l_{11}&=-J^{-1}B(q,\overline{q})\\
&=\frac{2}{(afh+bdl)(a^2+\alpha_2)(l^2+\alpha_2)}(b(h(b_{011}l^2+c_{002}fh-c_{011}fl)a^2+(a_{110}fh+bb_{110}l)(l^2\\
&+\alpha_2)a+\alpha_2h(b_{011}l^2+c_{002}fh-c_{011}fl)),-a(b(ab_{110}-a_{110}d)l^3+hb_{011}(a^2+\alpha_2)l^2\\
&+(-a^2c_{011}fh+\alpha_2bb_{110}a-\alpha_2(da_{110}b+c_{011}fh))l+c_{002}fh^2(a^2+\alpha_2)),(a^3b_{011}hl-b(\\
&-b_{110}l^2+c_{002}dh-c_{011}dl-\alpha_2b_{110})a^2+a(-da_{110}(l^2+\alpha_2)b+\alpha_2hlb_{011})-\alpha_2bd(c_{002}h\\
&-c_{011}l))h)^{\mathrm{T}},\\
l_{20}&=(2i\sqrt{\alpha_2}I_3-J)^{-1}B(q,q)\\
&=\frac{1}{-8i\alpha_2^{\frac{3}{2}}+(2al-2bd-2fh)i\sqrt{\alpha_2}+(db+4\alpha_2)l+afh+4\alpha_2a}(\frac{2(-2i\sqrt{\alpha_2}l-fh-4\alpha_2)a_{110}b}{i\sqrt{\alpha_2}-a}\\
&+b(2i\sqrt{\alpha_2}-l)(\frac{2b_{110}b}{i\sqrt{\alpha_2}-a}+\frac{2b_{011}h}{i\sqrt{\alpha_2}-l})+bf(\frac{2c_{011}h}{i\sqrt{\alpha_2}-l}+\frac{2c_{002}h^2}{(i\sqrt{\alpha_2}-l)^2}),\frac{2d(2i\sqrt{\alpha_2}-l)a_{110}b}{i\sqrt{\alpha_2}-a}\\
&+(2i\sqrt{\alpha_2}-a)(2i\sqrt{\alpha_2}-l)(\frac{2b_{110}b}{i\sqrt{\alpha_2}-a}+\frac{2b_{011}h}{i\sqrt{\alpha_2}-l})+(2i\sqrt{\alpha_2}-a)f(\frac{2c_{011}h}{i\sqrt{\alpha_2}-l}+\frac{2c_{002}h^2}{(i\sqrt{\alpha_2}-l)^2}),\\
&\frac{2dha_{110}b}{i\sqrt{\alpha_2}-a}+(2i\sqrt{\alpha_2}-a)h(\frac{2b_{110}b}{i\sqrt{\alpha_2}-a}+\frac{2b_{011}h}{i\sqrt{\alpha_2}-l})+(-4\alpha_2-2i\sqrt{\alpha_2}a-db)(\frac{2c_{011}h}{i\sqrt{\alpha_2}-l}+\frac{2c_{002}h^2}{(i\sqrt{\alpha_2}-l)^2}))^{\mathrm{T}},
\end{aligned}$$

where I_3 is the 3×3 unit matrix, and the first Lyapunov coefficient l_1 is given by

$$l_1=\frac{1}{\sqrt{\alpha_2}}\mathrm{Re}(C_1),$$

where

$$C_1=\frac{1}{2}\langle p,C(q,q,\overline{q})+B(\overline{q},l_{20})+2B(q,l_{11})\rangle.$$

If $l_1 = 0$, the model (1.1) may occur generalized Hopf bifurcation, the second Lyapunov coefficient l_2 can be calculated by the following form

$$l_2 = \frac{1}{\sqrt{\alpha_2}}\mathrm{Re}(C_2),$$

where

$$\begin{aligned} C_2 = \frac{1}{12}\langle p, E(q,q,q,\overline{q},\overline{q}) + D(q,q,q,\bar{l}_{20}) + 3D(q,\overline{q},\overline{q},l_{20}) + 6D(q,q,\overline{q},l_{11}) + C(\overline{q},\overline{q},l_{30}) \\ + 3C(q,q,\bar{l}_{21}) + 6C(q,\overline{q},l_{21}) + 3C(q,\bar{l}_{20},l_{20}) + 6C(q,l_{11},l_{11}) + 6C(\overline{q},l_{20},l_{11}) \\ + 2B(\overline{q},l_{31}) + 3B(q,l_{22}) + B(\bar{l}_{20},l_{30}) + 3B(\bar{l}_{21},l_{20}) + 6B(l_{11},l_{21})\rangle, \end{aligned}$$

and

$$\begin{aligned} l_{20} &= (2i\sqrt{\alpha_2}I_3 - J)^{-1}B(q,q), \\ l_{11} &= -J^{-1}B(q,\overline{q}), \\ l_{30} &= (3i\sqrt{\alpha_2}I_3 - J)^{-1}[C(q,q,q) + 3B(q,l_{20})], \\ l_{21} &= (i\sqrt{\alpha_2}I_3 - J)^{-1}[C(q,q,\overline{q}) + B(\overline{q},l_{20}) + 2B(q,l_{11}) - 2C_1 q], \\ l_{31} &= (2i\sqrt{\alpha_2}I_3 - J)^{-1}[D(q,q,q,\overline{q}) + 3C(q,q,l_{11}) + 3C(q,\overline{q},l_{20}) \\ &\quad + 3B(l_{20},l_{11}) + B(\overline{q},l_{30}) + 3B(q,l_{21}) - 6C_1 l_{20}], \\ l_{22} &= -J^{-1}[D(q,q,\overline{q},\overline{q}) + 4C(q,\overline{q},l_{11}) + C(\overline{q},\overline{q},l_{20}) + C(q,q,\bar{l}_{20}) \\ &\quad + 2B(l_{11},l_{11}) + 2B(q,\bar{l}_{21}) + 2B(\overline{q},l_{21}) + B(\bar{l}_{20},l_{20}) - 4l_{11}(C_1 + \overline{C}_1)], \end{aligned}$$

where I_3 is the 3×3 unit matrix, and we do not present the long expressions of $l_{30}, l_{21}, l_{31}, l_{22}$.

Based on the above theoretical analysis, the following results are derived.

Theorem 4. For model (1.1), if $l_1 < 0$ (> 0), then the bifurcating periodic solutions are asymptotically stable (unstable); if $l_1 = 0$, then Hopf bifurcation is generalized.

3.2.3. Bogdanov-Takens bifurcation

According to Theorem 1, model (1.1) has two endemic equilibria E_1 and E_* when $\Delta = 0$. Furthermore, if $\alpha_2 = 0$, the eigenvalues of the Jacobian matrix J_{E_*} are $\lambda_{1,2} = 0$ and $\lambda_3 = -\alpha_1$, that is to say the model (1.1) may undergo a Bogdanov-Takens bifurcation. Therefore, the following results are given.

Theorem 5. Suppose that $\Delta = 0, \alpha_2 = 0, M_{20} \neq 0$. If $M_{11} + 2L_{20} \neq 0$, then E_* is a cusp point of codimension 2; if $M_{11} + 2L_{20} = 0$, E_* is at least a cusp point of codimension 3.

Proof. Introducing the following affine transformation

$$\begin{pmatrix} x \\ y \\ z \end{pmatrix} = \begin{pmatrix} \frac{-bl}{a} & -\frac{bl}{a^2} + \frac{b}{a} & \frac{ba}{l} \\ l & -1 & a \\ -h & 0 & h \end{pmatrix} \begin{pmatrix} u \\ v \\ w \end{pmatrix}, \tag{3.6}$$

where a, b, h, l are given in (3.1). Then system (3.4) takes the form

$$\begin{cases} \dot{u} = v + L_{20}u^2 + L_{11}uv + L_{02}v^2 + w \cdot O(|u, v|) + O(|u, v, w|^3), \\ \dot{v} = M_{20}u^2 + M_{11}uv + M_{02}v^2 + w \cdot O(|u, v|) + O(|u, v, w|^3), \\ \dot{w} = -\alpha_1 w + K_{20}u^2 + K_{11}uv + K_{02}v^2 + w \cdot O(|u, v|) + O(|u, v, w|^3), \end{cases} \tag{3.7}$$

where

$$\begin{aligned} L_{20} &= \frac{-al^3a_{110}}{(a-l)(l+a)^2} + \frac{l(-b_{011}lh - \frac{b_{110}bl^2}{a})}{(l+a)^2} - \frac{a(a^2+al-l^2)(c_{002}h^2 - c_{011}lh)}{h(a-l)(l+a)^2}, \\ L_{11} &= \frac{a^2l(a_{110}l(\frac{-bl}{a^2} + \frac{b}{a}) + \frac{a_{110}bl}{a})}{b(a-l)(a+l)^2} + \frac{l(b_{011}h + b_{110}l(\frac{-bl}{a^2} + \frac{b}{a}) + \frac{b_{110}lb}{a})}{(a+l)^2} \\ &\quad - \frac{a(a^2+al-l^2)c_{011}}{(a-l)(a+l)^2}, \\ L_{02} &= \frac{a^2la_{110}(\frac{bl}{a^2} - \frac{b}{a})}{b(a-l)(a+l)^2} + \frac{lb_{110}(\frac{bl}{a^2} - \frac{b}{a})}{(a+l)^2}, \\ M_{20} &= -\frac{a_{110}l^3a}{(a-l)(a+l)} - \frac{a(-b_{011}lh - \frac{b_{110}bl^2}{a})}{a+l} - \frac{a^2l(c_{002}h^2 - c_{011}hl)}{(a-l)(a+l)h}, \\ M_{11} &= \frac{-a^2l(a_{110}l(\frac{bl}{a^2} - \frac{b}{a}) - \frac{a_{110}bl}{a})}{b(a-l)(a+l)} - \frac{a^2lc_{011}}{(a-l)(a+l)} \\ &\quad + \frac{a(-b_{011}h + b_{110}l(\frac{bl}{a^2} - \frac{b}{a}) - \frac{b_{110}bl}{a})}{a+l}, \\ M_{02} &= \frac{a^2la_{110}(\frac{bl}{a^2} - \frac{b}{a})}{b(a-l)(a+l)} - \frac{ab_{110}(\frac{bl}{a^2} - \frac{b}{a})}{a+l}, \\ K_{20} &= L_{20} + c_{002}h - c_{011}l, \\ K_{11} &= L_{11} + c_{011}, \\ K_{02} &= L_{02}. \end{aligned}$$

Applying the center manifold theorem, system (3.7) becomes

$$\begin{cases} \dot{u} = v + L_{20}u^2 + L_{11}uv + L_{02}v^2 + O(|u, v|^3), \\ \dot{v} = M_{20}u^2 + M_{11}uv + M_{02}v^2 + O(|u, v|^3). \end{cases} \tag{3.8}$$

Using the following transformation

$$\begin{aligned} u &= \eta_1 + \frac{1}{2}(L_{11} + M_{02})\eta_1^2 + L_{02}\eta_1\eta_2 + O(|\eta_1, \eta_2|^3), \\ v &= \eta_2 - L_{20}\eta_1^2 + M_{02}\eta_1\eta_2 + O(|\eta_1, \eta_2|^3). \end{aligned}$$

It can be derived that

$$\begin{cases} \dot{\eta}_1 = \eta_2, \\ \dot{\eta}_2 = M_{20}\eta_1^2 + (M_{11} + 2L_{20})\eta_1\eta_2 + O(|\eta_1, \eta_2|^3). \end{cases} \tag{3.9}$$

Therefore, assumed that $\Delta = 0, \alpha_2 = 0, M_{20} \neq 0$. If $M_{11} + 2L_{20} \neq 0$, E_* is a cusp point of codimension 2, and the codimension of the cusp point is at least 3 if $M_{11} + 2L_{20} = 0$. □

In the following analysis, ϕ, c are chosen as bifurcation parameters, $\phi = \phi_0$ and $c = c_0$ satisfy $\Delta = 0$ and $\alpha_2 = 0$. The model (1.1) is perturbed with (ϕ, c) in a small neighborhood of (ϕ_0, c_0). Let $\phi = \phi_0 + \epsilon_1, c = c_0 + \epsilon_2$, where $\epsilon = (\epsilon_1, \epsilon_2)$ is a parameter vector in a small neighborhood of $(0, 0)$. By the translation $x = S - S^*, y = I - I^*, z = I_d - I_d^*$ and using Taylor expansion, model (1.1) is transformed into

$$\begin{cases} \frac{dx}{dt} = ax + by + a_{110}xy, \\ \frac{dy}{dt} = q^{'} + dx + e^{'}y + (f + f^{'})z + b_{110}xy + (b_{011} + b_{011}^{'})yz, \\ \frac{dz}{dt} = c^{'} + (h + h^{'})y + (l + l^{'})z + (c_{011} + c_{011}^{'})yz + (c_{002} + c_{002}^{'})z^2 + O(|z|^3), \end{cases} \tag{3.10}$$

where $a, b, a_{110}, d, f, b_{110}, b_{011}, h, l, c_{011}, c_{002}$ are given in system (3.4) and

$$\begin{aligned} & q^{'} = -m\epsilon_1 I^* I_d^*, \ \ e^{'} = -m\epsilon_1 I_d^*, \ \ f^{'} = -m\epsilon_1 I^*, \ \ b_{011}^{'} = -m\epsilon_1, \\ & c^{'} = m\epsilon_1 I^* I_d^* - \frac{\epsilon_2 I_d^*}{\alpha + I_d^*}, \quad h^{'} = m\epsilon_1 I_d^*, \quad c_{011}^{'} = m\epsilon_1, \\ & l^{'} = \frac{1}{(\alpha + I_d^*)^2}(\epsilon_1 I^* m(I_d^* + \alpha)^2 - \epsilon_2 \alpha), \ \ c_{002}^{'} = \frac{\epsilon_2 \alpha}{(\alpha + I_d^*)^3}. \end{aligned}$$

Applying the transformation (3.6), then system (3.10) restricted on the center manifold is

$$\begin{cases} \dot{u} = v + a_{00} + a_{10}u + a_{01}v + \frac{1}{2}a_{20}u^2 + a_{11}uv + \frac{1}{2}a_{02}v^2 + O(|u, v|^3), \\ \dot{v} = b_{00} + b_{10}u + b_{01}v + \frac{1}{2}b_{20}u^2 + b_{11}uv + \frac{1}{2}b_{02}v^2 + O(|u, v|^3), \end{cases} \tag{3.11}$$

where

$$\begin{aligned} a_{00} &= \frac{lq^{'}}{(a + l)^2} - \frac{a(a^2 + al - l^2)c^{'}}{h(a - l)(l + a)^2}, \\ a_{10} &= \frac{l(-\frac{dbl}{a} + e^{'}l - fh)}{(a + l)^2} - \frac{a(a^2 + al - l^2)((h + h^{'})l - (l + l^{'})h)}{h(a - l)(a + l)^2}, \\ a_{01} &= -\frac{e^{'}l}{(a + l)^2} + \frac{a(a^2 + al - l^2)h^{'}}{h(a - l)(a + l)^2}, \\ a_{20} &= 2L_{20} - 2\frac{b_{011}^{'}l^2 h}{(a + l)^2} - 2\frac{a(a^2 + al - l^2)(c_{002}^{'}h^2 - c_{011}^{'}lh)}{h(a - l)(a + l)^2}, \\ a_{11} &= L_{11} + \frac{l(\frac{blh}{a} + b_{011}^{'}h)}{(a + l)^2} - \frac{a(a^2 + al - l^2)c_{011}^{'}}{(a - l)(a + l)^2}, \\ a_{02} &= 2L_{02}, \\ b_{00} &= -\frac{aq^{'}}{a + l} - \frac{a^2 lc^{'}}{(a - l)h(a + l)}, \\ b_{10} &= -\frac{a(-\frac{dbl}{a} + e^{'}l - fh)}{a + l} - \frac{a^2 l((h + h^{'})l - (l + l^{'})h)}{(a - l)(a + l)h}, \\ b_{01} &= -\frac{al^2}{(a + l)(a - l)} + \frac{a^2 e^{'} - bda + bdl}{a(a + l)} + \frac{a^2 l(h + h^{'})}{(a + l)(a - l)h}, \\ b_{20} &= 2M_{20} + 2\frac{a(b_{011}^{'}lh)}{a + l} - 2\frac{a^2 l(-c_{011}^{'}lh + c_{002}^{'}h^2)}{(a - l)(a + l)h}, \end{aligned}$$

$$b_{11} = M_{11} + \frac{a(\frac{-blh}{a} - b_{011}^{'}h)}{a+l} - \frac{a^2 lc_{011}^{'}}{(a+l)(a-l)},$$
$$b_{02} = 2M_{02}.$$

Define a nonlinear transformation

$$x = u,$$
$$y = v + a_{00} + a_{10}u + a_{01}v + \frac{1}{2}a_{20}u^2 + a_{11}uv + \frac{1}{2}a_{02}v^2 + O(|u,v|^3).$$

It can be derived from system (3.11) that

$$\begin{cases} \dot{x} = y, \\ \dot{y} = g_{00} + g_{10}x + g_{01}y + \frac{1}{2}g_{20}x^2 + g_{11}xy + \frac{1}{2}g_{02}y^2 + O(|x,y|^3), \end{cases} \tag{3.12}$$

where

$$\begin{aligned} g_{00} &= b_{00} + O(\epsilon^2), \\ g_{10} &= b_{10} + a_{11}b_{00} - b_{11}a_{00} + O(\epsilon^2), \\ g_{01} &= b_{01} + a_{10} + a_{02}b_{00} - (a_{11} + b_{02})a_{00} + O(\epsilon^2), \\ g_{20} &= b_{20} + O(\epsilon), \\ g_{11} &= a_{20} + b_{11} + O(\epsilon), \\ g_{02} &= b_{02} + 2a_{11} + O(\epsilon). \end{aligned}$$

Introducing the transformation

$$x = v_1 - \frac{g_{01}}{g_{11}}, \quad y = v_2.$$

One can obtain

$$\begin{cases} \dot{v_1} = v_2, \\ \dot{v_2} = h_{00} + h_{10}v_1 + \frac{1}{2}h_{20}v_1^2 + h_{11}v_1v_2 + \frac{1}{2}h_{02}v_2^2 + O(|v_1,v_2|^3), \end{cases} \tag{3.13}$$

where

$$\begin{aligned} h_{00} &= g_{00} - \frac{g_{01}}{g_{11}}g_{10} + O(\epsilon^2), \\ h_{20} &= g_{20} + O(\epsilon), \\ h_{10} &= g_{10} - \frac{g_{01}}{g_{11}}g_{20} + O(\epsilon^2), \\ h_{11} &= g_{11} + O(\epsilon), \\ h_{02} &= g_{02} + O(\epsilon). \end{aligned}$$

Introducing a new time variable τ by $\mathrm{d}t = (1 - \frac{h_{02}}{2}v_1)\mathrm{d}\tau$ and rewriting τ as t. Then

$$\begin{cases} \dot{v_1} = v_2 - \frac{h_{02}}{2}v_1v_2, \\ \dot{v_2} = h_{00} + (h_{10} - \frac{h_{02}}{2}h_{00})v_1 + \frac{1}{2}(h_{20} - h_{02}h_{10})v_1^2 \\ \quad + h_{11}v_1v_2 + \frac{1}{2}h_{02}v_2^2 + O(|v_1,v_2|^3). \end{cases} \tag{3.14}$$

Using the transformation

$$\xi_1 = v_1,\ \xi_2 = v_2 - \frac{h_{02}}{2}v_1v_2,$$

system (3.14) becomes

$$\begin{cases}\dot{\xi}_1 = \xi_2,\\ \dot{\xi}_2 = \mu_1 + \mu_2\xi_1 + \mu_3\xi_1^2 + \mu_4\xi_1\xi_2 + O(|\xi_1,\xi_2|^3),\end{cases} \tag{3.15}$$

where

$$\mu_1 = h_{00},\ \mu_2 = h_{10} - \frac{1}{2}h_{00}h_{02},\ \mu_3 = \frac{1}{2}(h_{20} - h_{10}h_{02}),\ \mu_4 = h_{11}.$$

Introducing the change of variables and rescaling of time

$$\eta_1 = \frac{\mu_4^2}{\mu_3}\xi_1,\ \eta_2 = \text{sign}(\frac{\mu_3}{\mu_4})\frac{\mu_4^3}{\mu_3^2}\xi_2,\ t = \left|\frac{\mu_3}{\mu_4}\right|\tau.$$

Then system (3.15) takes the required form

$$\begin{cases}\dot{\eta}_1 = \eta_2,\\ \dot{\eta}_2 = \beta_1 + \beta_2\eta_1 + \eta_1^2 + s\eta_1\eta_2 + O(|\eta_1,\eta_2|^3),\end{cases} \tag{3.16}$$

where

$$\beta_1 = \frac{\mu_4^4}{\mu_3^3}\mu_1,\ \beta_2 = \frac{\mu_4^2}{\mu_3^2}\mu_2,\ s = \text{sign}(\frac{\mu_4}{\mu_3}).$$

Next, a numerical example is proposed to show Bogdanov-Takens bifurcation. Taking $\phi = 0.05558, c = 3.69082$, other parameters are given in (4.1). By simple calculation, it can be obtained that

$$\begin{aligned}\beta_1 &= (1.6710\epsilon_2 - 14.134\epsilon_1)(-0.0011511 + 0.0030950\epsilon_1 - 9.6342\times10^{-7}\epsilon_2)^7\\ &\quad/(-0.00010783\epsilon_1^3 + 0.000022199\epsilon_1^4 + 1.7360\times10^{-8}\epsilon_2 - 7.3281\times10^{-7}\epsilon_1\epsilon_2\\ &\quad + 0.000042818\epsilon_1^2 + 2.6542\times10^{-6}\epsilon_1^2\epsilon_2 - 2.5058\times10^{-6}\epsilon_1^3\epsilon_2 + 1.4214\\ &\quad\times10^{-11}\epsilon_2^2 - 5.8151\times10^{-10}\epsilon_1\epsilon_2^2 + 1.4172\times10^{-9}\epsilon_1^2\epsilon_2^2 - 1.0591\times10^{-6}\epsilon_1 - 1.1977\times10^{-9})^3,\\ \beta_2 &= (-0.0011511 + 0.0030950\epsilon_1 - 9.6342\times10^{-7}\epsilon_2)^4(0.000075528\epsilon_1^3 - 2.9602\\ &\quad\times10^{-5}\epsilon_2 - 0.0045697\epsilon_1^2 + 0.000074794\epsilon_1\epsilon_2 - 3.1634\times10^{-6}\epsilon_1^2\epsilon_2 - 2.4213\\ &\quad\times10^{-8}\epsilon_2^2 + 3.0469\times10^{-8}\epsilon_1\epsilon_2^2 + 0.0018344\epsilon_1 - 2.3246\times10^{-8})/(-1.0783\\ &\quad\times10^{-4}\epsilon_1^3 + 0.000022199\epsilon_1^4 + 1.7360\times10^{-8}\epsilon_2 - 7.3281\times10^{-7}\epsilon_1\epsilon_2 + 4.2818\\ &\quad\times10^{-5}\epsilon_1^2 + 2.6542\times10^{-6}\epsilon_1^2\epsilon_2 - 2.5058\times10^{-6}\epsilon_1^3\epsilon_2 + 1.4214\times10^{-11}\epsilon_2^2\\ &\quad - 5.8151\times10^{-10}\epsilon_1\epsilon_2^2 + 1.4172\times10^{-9}\epsilon_1^2\epsilon_2^2 - 1.0591\times10^{-6}\epsilon_1 - 1.1977\\ &\quad\times10^{-9})^2\times(-0.0011511 + 0.0030950\epsilon_1 - 9.6342\times10^{-7}\epsilon_2),\end{aligned}$$

then

$$\left|\frac{\partial(\beta_1(\epsilon),\beta_2(\epsilon))}{\partial(\epsilon_1,\epsilon_2)}\right|_{\epsilon=0} = 4.4863 \times 10^{12}.$$

Therefore, model (1.1) undergoes a Bogdanov-Takens bifurcation of codimension 2 in a small neighborhood of (ϕ_0, c_0). According to Lemma 8.7 in Kuznetsov [17], the following Theorem can be obtained.

Theorem 6. For model (1.1), we take ϕ and c as bifurcation parameters, the bifurcation cures are given by the following:
1) Saddle-node bifurcation occurs from the bifurcation curve:

$$SN = \left\{(\epsilon_1, \epsilon_2) : 4\beta_1 = \beta_2^2\right\};$$

2) Hopf bifurcation occurs from the bifurcation curve:

$$H = \{(\epsilon_1, \epsilon_2) : \beta_1 = 0, \beta_2 < 0\};$$

3) Homoclinic orbit occurs from the bifurcation curve:

$$HL = \left\{(\epsilon_1, \epsilon_2) : 25\beta_1 + 6\beta_2^2 \approx 0, \beta_2 < 0\right\}.$$

4. Numerical simulation

In this section, the theoretical conclusions of model (1.1) are validated by the numerical simulation. The following data are used for numerical analysis in the full text.

$$A = 5,\ \beta = 0.003,\ \mu = 0.01,\ \sigma = 0.01,\ m = 0.02,\ \alpha = 0.5. \tag{4.1}$$

In Figure 1, it is easy to see that the model (1.1) may exist one or three positive equilibria as the change of σ. In addition, there are two limit points for model (1.1), that is, the model (1.1) undergoes saddle-node bifurcation.

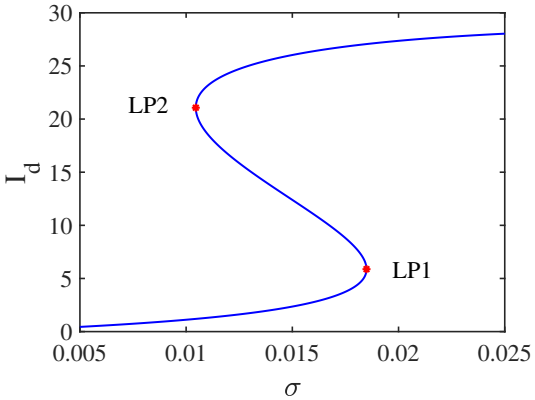

Figure 1. Existence of saddle-node bifurcation at $LP1$ and $LP2$ when $\sigma = 0.018492(W^T[D^2 F(E_*;\sigma^*)\ (V,V)] = 2.422 \times 10^{-6})$ and $\sigma = 0.010455(W^T[D^2F(E_*;\sigma^*)(V,V)] = -8.303 \times 10^{-7})$. Where $A = 5, \beta = 0.003, \mu = 0.01, m = 0.02, \phi = 0.13, c = 4, \alpha = 0.5$.

The bifurcation curve of co-dimension 1 of model (1.1) is given in Figure 2(a). Taking c as the bifurcation parameter, there are two Hopf points and two limit points with the change of c. When $c = 3.81680$, $E_1(\lambda_1 = -0.6, \lambda_{2,3} = -0.0003 \pm 0.08i)$ and $E_3(\lambda_{1,2} = -0.01 \pm 0.1i, \lambda_3 = -0.01)$ are stable foci, E_2 is a saddle point and an unstable limit cycle ($l_1 = 2.1206 \times 10^{-5} > 0$) emerges from the Hopf point (H1) near the equilibrium E_1, which is illustrated in Figure 3(a),(b). If $c = 3.92610$, $E_1(\lambda_1 = -0.6, \lambda_{2,3} = -0.07 \pm 0.07i)$ and $E_3(\lambda_{1,2} = -0.01 \pm 0.1i, \lambda_3 = -0.01)$ are also stable foci, E_2 is a saddle point and an unstable limit cycle ($l_1 = 3.1916 \times 10^{-5} > 0$) arises from the Hopf point (H2) near the equilibrium E_3, it is shown in Figure 3(c),(d).

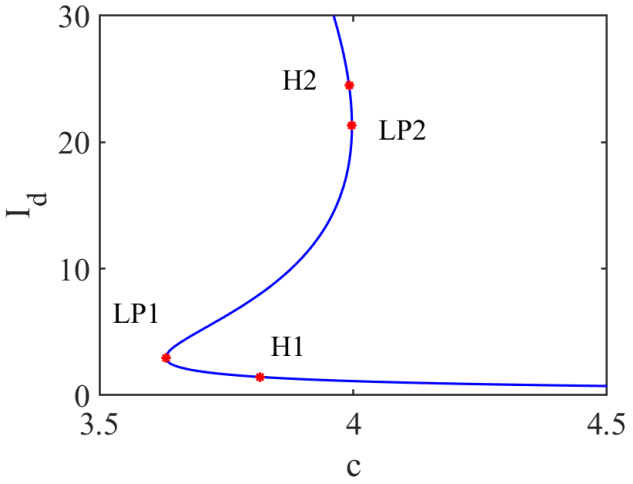

(a) Other parameters are fixed except $c(\phi = 0.13)$, Hopf bifurcation curve is given in (c, I_d) plane.

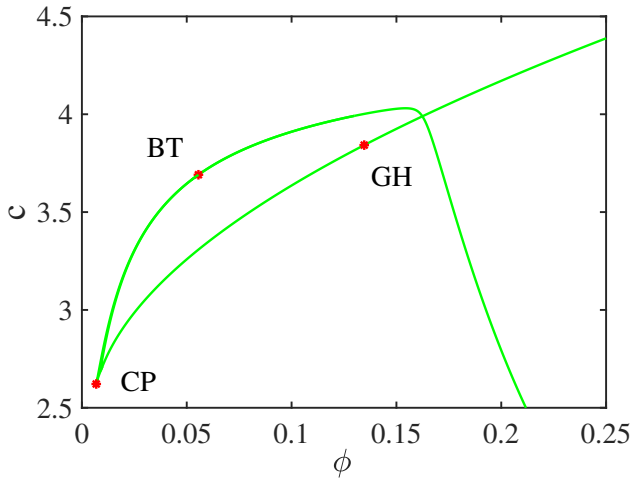

(b) Other parameters are fixed except ϕ and c, 2-codimension bifurcation curves can be obtained in (ϕ, c) plane.

Figure 2. Bifurcation diagram of the model (1.1).

The bifurcation curves of co-dimension 2 are generated from Figure 2(b), one of them shows a generalized Hopf bifurcation (GH) and the other is a Bogdanov-Takens bifurcation (BT). In Figure 3(e),

$E_3(\lambda_{1,2} = -0.01 \pm 0.1i, \lambda_3 = -0.01)$ is locally stable and E_2 is a saddle point, the Bautin (generalized Hopf) bifurcation ($l_1 = 0, l_2 = -6.9961 \times 10^{-6} < 0$) occurs at $(\phi, c) = (0.13458, 3.84246)$. There are two limit cycles that appear near equilibrium E_1, and the large limit cycle is stable and the small one is unstable, the phase portrait is illustrated in Figure 3(f). In Figure 4(a),(b), $E_1(\lambda_1 = -0.03, \lambda_2 = -0.7, \lambda_3 = -0.4)$ is a stable node and E_* is a BT point of order 2. As shown in Figure 4(c),(d),(e),(f), with the values of ϕ and c increase, E_1 is still a stable node and E_3 is a stable focus, the model first appears an unstable limit cycle around E_3, then the limit cycle disappears, model (1.1) has a homoclinic orbit to the saddle point E_2 and it eventually disappears.

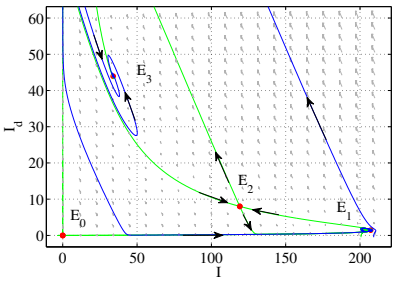

(a) A limit cycle near the equilibrium E_1 with $\phi = 0.13, c = 3.81680$.

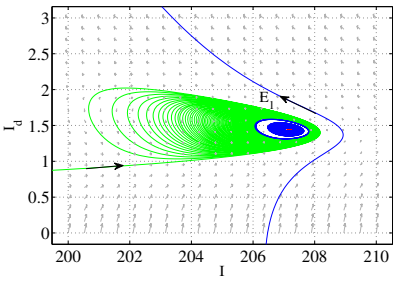

(b) The limit cycle is shown by enlarging the phase diagram around E_1.

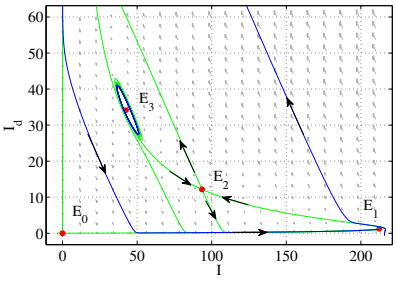

(c) A limit cycle near the equilibrium E_3 with $\phi = 0.13, c = 3.92610$.

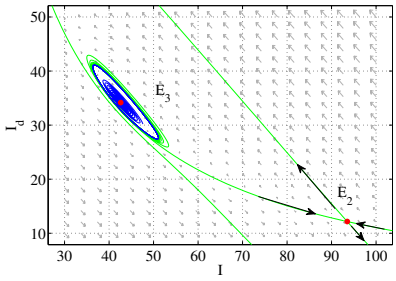

(d) The local enlarged view of the limit cycle.

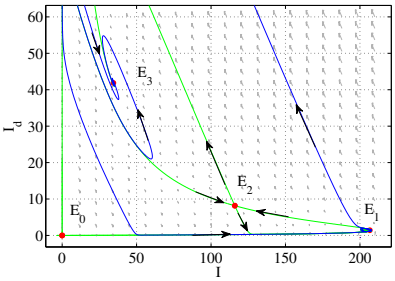

(e) Two limit cycles near the equilibrium E_1 with $\phi = 0.13458$, $c = 3.84246$.

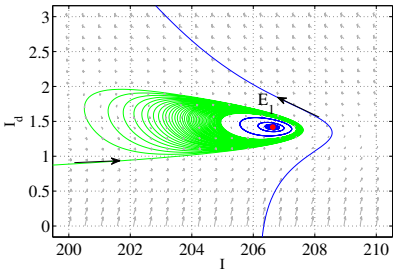

(f) Partial enlarged views of the two limit cycles.

Figure 3. The phase portraits of model (1.1) with different parameter values.

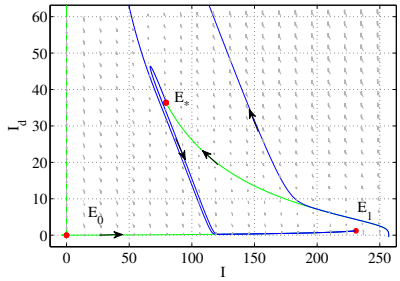

(a) E_* is the Bogdanov-Takens point of order 2 with $\phi = 0.05558, c = 3.69082$.

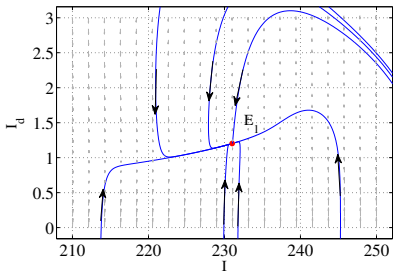

(b) A local enlarged view around E_1 with $\phi = 0.05558, c = 3.69082$.

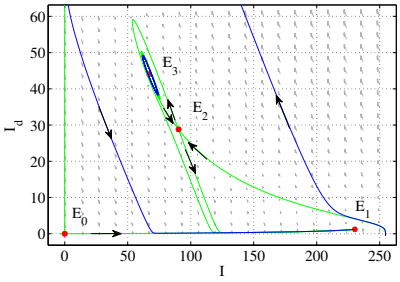

(c) A limit cycle near the equilibrium E_3 is given with $\phi = 0.05795, c = 3.69372$.

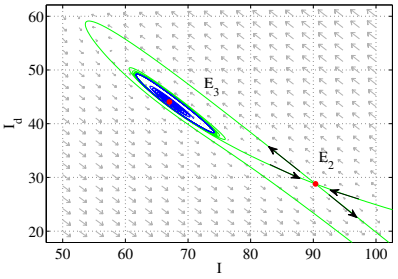

(d) The limit cycle is shown by enlarging the phase diagram around E_3.

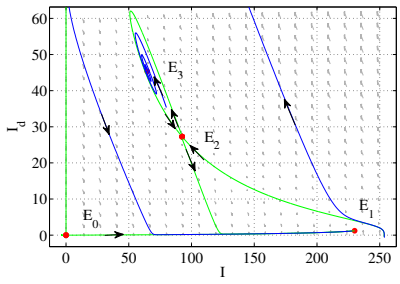

(e) Model (1.1) has a homoclinic orbit to the saddle point E_2 with $\phi = 0.05897, c = 3.69477$.

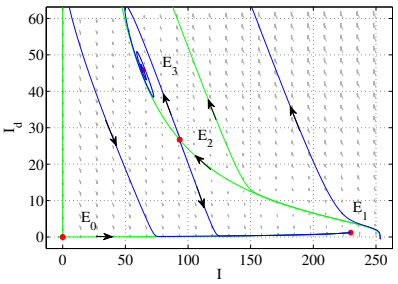

(f) Model (1.1) has two locally stable equilibria E_1 and E_3, a unstable DFE E_0 and a saddle E_2 with $\phi = 0.05941, c = 3.69520$.

Figure 4. The phase portraits near the codimension-2 Bogdanov-Takens bifurcation.

5. Conclusions and discussion

Testing-culling is a major prevention and control measure for brucellosis used by the animal disease regulatory authorities of some countries [8, 18]. Therefore, the impact of testing and culling measures is an interesting research topic. In this paper, on the basis of brucellosis control policies and the characteristics of animal testing and considering the limitation of culling resources, a mathematical model is established to demonstrate the impact of testing and culling measures on the dynamics of brucellosis transmission. The model is found to have a disease-free equilibrium that is globally asymptotically stable if $R_0 \leq 1$, and there may be one or three positive equilibria if $R_0 > 1$,

which leads to saddle-node bifurcation, (generalized) Hopf bifurcation and Bogdanov-Takens bifurcation in the model. Biologically speaking, saddle node bifurcation means that the model appears multi-stable; that is, the initial state of each subpopulation may affect the level of brucellosis transmission. The Hopf bifurcation and Bogdanov-Takens bifurcation imply that the model undergoes periodic oscillations. In other words, if the epidemic is at the lowest point of the cycle, it prompts people to think that the disease may disappear, affecting the implementation of prevention and control measures. In addition, the endemic equilibrium of the model is globally asymptotically stable if no testing and culling are conducted, which implies that testing and culling measures can lead to complex dynamics of brucellosis transmission.

Our study has some limitations. Some features of animal culling are still not considered in the model. For example, the disease may spread because of the delayed culling of infected animals. Further, in practice, because of the sensitivity of the test reagents, the test results need to be reconfirmed, and this test process is also not expressed in our model. We need to further consider these aspects.

Acknowledgments

This research is partially supported by the Fundamental Research Program of Shanxi Province (20210302123031,20210302123019), the National Youth Science Foundation of China (11501528).

Conflict of interest

The authors declare there is no conflict of interest.

References

1. T. Barbier, F. Collard, A. Zúñiga-Ripa, I. Moriyón, T. Godard, J. Becker, et al., Erythritol feeds the pentose phosphate pathway via three new isomerases leading to D-erythrose-4-phosphate in Brucella, *Proc. Natl. Acad. Sci. U. S. A.*, **111** (2014), 17815–17820. https://doi.org/10.1073/pnas.1414622111
2. P. Andriopoulos, M. Tsironi, S. Deftereos, A. Aessopos, G. Assimakopoulos, Acute brucellosis: Presentation, diagnosis, and treatment of 144 cases, *Int. J. Infect. Dis.*, **11** (2007), 52–57. https://doi.org/10.1016/j.ijid.2005.10.011
3. G. Pappas, P. Papadimitriou, N. Akritidis, L. Christou, E. V. Tsianos, The new global map of human brucellosis, *Lancet Infect. Dis.*, **6** (2006), 91–99. https://doi.org/10.1016/S1473-3099(06)70382-6
4. H. Zeng, Y. M. Wang, X. D. Sun, P. Liu, Q. G. Xu, D. Huang, et al., Status and influencing factors of farmers' private investment in the prevention and control of sheep brucellosis in China: A cross-sectional study, *PLoS Neglected Trop. Dis.*, **13** (2019), e0007285. https://doi.org/10.1371/journal.pntd.0007285
5. A. J. S. Alves, F. Rocha, M. Amaku, F. Ferreira, E. O. Telles, J. H. H. Grisi Filho, et al., Economic analysis of vaccination to control bovine brucellosis in the States of Sao Paulo and Mato Grosso, Brazil, *Prev. Vet. Med.*, **118** (2015), 351–358. https://doi.org/10.1016/j.prevetmed.2014.12.010

6. Q. Hou, X. D. Sun, J. Zhang, Y. J. Liu, Y. M. Wang, Z. Jin, Modeling the transmission dynamics of sheep brucellosis in Inner Mongolia Autonomous Region, China, *Math. Biosci.*, **242** (2013), 51–58. https://doi.org/10.1016/j.mbs.2012.11.012
7. H. Yoon, O. K. Moon, S. H. Lee, W. C. Lee, M. Her, W. Jeong, et al., Epidemiology of brucellosis among cattle in Korea from 2001 to 2011, *J. Vet. Sci.*, **15** (2014), 537–543. https://doi.org/10.4142/jvs.2014.15.4.537
8. R. M. Davidson, Control and eradication of animal diseases in New Zealand, *N. Z. Vet. J.*, **50** (2002), 6–12. https://doi.org/10.1080/00480169.2002.36259
9. M. Zamri-Saad, M. I. Kamarudin, Control of animal brucellosis: The Malaysian experience, *Asian Pac. J. Trop. Med.*, **9** (2016), 1136–1140. https://doi.org/10.1016/j.apjtm.2016.11.007
10. N. Zhang, D. S. Huang, W. Wu, J. Liu, F. Liang, B. S. Zhou, et al., Animal brucellosis control or eradication programs worldwide: A systematic review of experiences and lessons learned, *Prev. Vet. Med.*, **160** (2018), 105–115. https://doi.org/10.1016/j.prevetmed.2018.10.002
11. P. O. Lolika, C. Modnak, S. Mushayabasa, On the dynamics of brucellosis infection in bison population with vertical transmission and culling, *Math. Biosci.*, **305** (2018), 42–54. https://doi.org/10.1016/j.mbs.2018.08.009
12. L. Bolzoni, R. D. Marca, M. Groppi, A. Gragnani, Dynamics of a metapopulation epidemic model with localized culling, *Discrete Cont. Dyn.-B*, **25** (2020), 2307–2330. https://doi.org/10.3934/dcdsb.2020036
13. J. Zinsstag, F. Roth, D. Orkhon, G. Chimed-Ochir, M. Nansalmaa, J. Kolar, et al., A model of animal-human brucellosis transmission in Mongolia, *Prev. Vet. Med.*, **69** (2005), 77–95. https://doi.org/10.1016/j.prevetmed.2005.01.017
14. M. F. Abakar, H. Yahyaoui Azami, P. Justus Bless, L. Crump, P. Lohmann, M. Laager, et al., Transmission dynamics and elimination potential of zoonotic tuberculosis in morocco, *PLoS Neglected Trop. Dis.*, **11** (2017), e0005214. https://doi.org/10.1371/journal.pntd.0005214
15. P. van den Driessche, J. Watmough, Reproduction numbers and sub-threshold endemic equilibria for compartmental models of disease transmission, *Math. Biosci.*, **180** (2002), 29–48. https://doi.org/10.1016/S0025-5564(02)00108-6
16. G. H. Li, Y. X. Zhang, Dynamic behaviors of a modified SIR model in epidemic diseases using nonlinear incidence and recovery rates, *PLoS One*, **12** (2017), e0175789. https://doi.org/10.1371/journal.pone.0175789
17. Y. A. Kuznetsov, *Elements of Applied Bifurcation Theory*, 3^{rd} edition, Springer-Verlag, New York, 2004. https://doi.org/10.1007/978-1-4757-3978-7
18. D. A. Abernethy, J. Moscard-Costello, E. Dickson, R. Harwood, K. Burns, E. McKillop, et al., Epidemiology and management of a bovine brucellosis cluster in Northern Ireland, *Prev. Vet. Med.*, **98** (2011), 223–229. https://doi.org/10.1016/j.prevetmed.2010.11.002

AIMS Press